Pharmaceutical Research, Vol. 26, No. 8, August 2009 (© 2009)
DOI: 10.1007/s11095-009-9896-0

Research Paper

Identification of Novel Specific and General Inhibitors of the Three Major Human ATP-Binding Cassette Transporters P-gp, BCRP and MRP2 Among Registered Drugs

Pär Matsson,[1] Jenny M. Pedersen,[1] Ulf Norinder,[1,2] Christel A. S. Bergström,[1] and Per Artursson[1,3]

Received March 8, 2009; accepted April 11, 2009; published online May 7, 2009

Purpose. To study the inhibition patterns of the three major human ABC transporters P-gp (ABCB1), BCRP (ABCG2) and MRP2 (ABCC2), using a dataset of 122 structurally diverse drugs.
Methods. Inhibition was investigated in cellular and vesicular systems over-expressing single transporters. Computational models discriminating either single or general inhibitors from non-inhibitors were developed using multivariate statistics.
Results. Specific (n=23) and overlapping (n=19) inhibitors of the three ABC transporters were identified. GF120918 and Ko143 were verified to specifically inhibit P-gp/BCRP and BCRP in defined concentration intervals, whereas the MRP inhibitor MK571 was revealed to inhibit all three transporters within one log unit of concentration. Virtual docking experiments showed that MK571 binds to the ATP catalytic site, which could contribute to its multi-specific inhibition profile. A computational model predicting general ABC inhibition correctly classified 80% of both ABC transporter inhibitors and non-inhibitors in an external test set.
Conclusions. The inhibitor specificities of P-gp, BCRP and MRP2 were shown to be highly overlapping. General ABC inhibitors were more lipophilic and aromatic than specific inhibitors and non-inhibitors. The identified specific inhibitors can be used to delineate transport processes in complex experimental systems, whereas the multi-specific inhibitors are useful in primary ABC transporter screening in drug discovery settings.

KEY WORDS: ABC transporters; drug transport; inhibition; structure–activity relationships; transport proteins.

INTRODUCTION

ATP-Binding Cassette (ABC) transporters are membrane proteins that mediate energy-dependent translocation of substrates across cellular membranes, with the potential of significantly affecting the disposition of drugs in tissues throughout the body (1,2). While some ABC transporters seem to be relatively specific for their endogenous substrates, others, including P-glycoprotein (P-gp/ABCB1), Breast Cancer Resistance Protein (BCRP/ABCG2), and Multidrug Resistance-Associated Protein 2 (MRP2/ABCC2), exhibit broad substrate specificities for a variety of drugs, toxins, metabolites and endogenous compounds (2–4).

In the intestine, these transporters are the three major proteins mediating efflux of drug-like compounds to the intestinal lumen, thereby limiting the intestinal absorption of foreign substances (5,6). A corresponding role in tissue detoxification is seen in the liver, where P-gp, BCRP and MRP2 are co-localized to the canalicular membrane and mediate the secretion of drugs and metabolites to bile (7–9). Consequently, inhibition of these transporters can lead to serious adverse effects, for instance through the accumulation of toxic drugs and metabolites in the liver (10,11), or by allowing drugs to access tissues that are normally protected, such as the brain or the placenta (12–16).

P-gp is the most well-studied member of the ABC transporter family and has been shown to transport substrates of high structural diversity (17–20). Owing to this promiscuity, describing the structural requirements for interaction with the transporting binding site with a single pharmacophore model has proven difficult (18,19,21). One reason for this could be the existence of several, partly overlapping binding sites in P-gp (22–25). Defining the exact binding mechanism of P-gp and related proteins is also hampered by the lack of high-resolution

Electronic supplementary material The online version of this article (doi:10.1007/s11095-009-9896-0) contains supplementary material, which is available to authorized users.

[1] Pharmaceutical Screening and Informatics, Department of Pharmacy, Uppsala University, P.O. Box 580, 751 23, Uppsala, Sweden.
[2] AstraZeneca R&D, Södertälje, Sweden.
[3] To whom correspondence should be addressed. (e-mail: Per.Artursson@farmaci.uu.se)

ABBREVIATIONS: ABC, ATP-binding cassette transporter; BCRP, Breast cancer resistance protein (ABCG2); BSEP, Bile salt efflux pump (ABCB11); $\log D_{7.4}$, Octanol–water partition coefficient at pH 7.4; HBSS, Hank's balanced salt solution; MRP2, Multidrug resistance associated protein 2 (ABCC2); PBS, Phosphate-buffered saline; P-gp, P-glycoprotein (ABCB1); PLS-DA, Partial least squares projection to latent structures discriminant analysis.

crystal structures for human ABC transporters (25–27).[1] Although several homology models based on bacterial ABC transporters have been presented for P-gp (28–33), sequence identity with the bacterial transporters used as templates is primarily found in the ATP-binding domains. In contrast, the transmembrane domains that contain the ligand recognition sites exhibit larger variations between the bacterial and human transporters, making high-precision modeling of these regions more difficult.

Ligand-based approaches have demonstrated that P-gp substrates and inhibitors are generally of a lipophilic nature and contain hydrogen bond acceptors or basic functionalities (20,30). It is generally accepted that the ligands access the P-gp binding site from within the plasma membrane bilayer, explaining the transporter's preference for lipophilic compounds (30,34,35). We recently observed a similar preference towards lipophilic inhibitors for BCRP (36), whereas both lipophilic cationic compounds and relatively hydrophilic and often negatively charged compounds were found among MRP2 inhibitors (37), suggesting the involvement of different binding sites (38). These results indicate that the structural requirements for inhibition of the three major human ABC transporters, P-gp, BCRP and MRP2 may be at least partly similar. However, knowledge gained so far of the affinity overlap between ABC transporters has been derived from scattered observations for individual compounds or small series (*e.g.*, 39–43). Therefore, more systematic studies of affinity patterns and the molecular features determining inhibition specificity are of interest.

In this paper, we studied the specificity pattern of inhibition for the three major human ABC transporters P-gp (ABCB1), BCRP (ABCG2) and MRP2 (ABCC2) using a dataset of 122 structurally diverse drugs tested at a single concentration. Specific and general inhibitors (n=23 and 19, respectively) of the three ABC transporters were identified, and concentration-dependent inhibition experiments conducted for nine selected compounds confirmed these results. Structural characteristics of the inhibitors of each transporter, as well as of compounds with general ABC transporter affinity, were determined using computational modeling techniques designed to discriminate transporter inhibitors from non-inhibitors.

MATERIALS AND METHODS

Materials

Fumitremorgin C was kindly provided by Dr. Robert Robey of the National Institutes of Health, Bethesda, MD. Ko143 was a kind gift from Dr. Gerrit-Jan Koomen of the Van't Hoff Institute for Molecular Sciences, University of Amsterdam, the Netherlands. All other compounds were purchased from Sigma-Aldrich, St. Louis, MO, and were of at least 95% purity.

Dataset Selection

The 122 compounds included in the dataset were selected to be structurally diverse and to represent the major part of the chemical space of registered oral drugs. All compounds were examined for transport inhibition in all of the three investigated proteins. BCRP inhibition data for 81 compounds were obtained from Matsson *et al.* (36), and were complemented with 41 new determinations in this study. The MRP2 inhibition data included in the present investigation were recently reported in Pedersen *et al.* (37). The P-gp data presented in Table I were obtained from the extensive literature on this well-studied ABC transporter, whereas the concentration dependent inhibition was determined experimentally as part of this study. The wealth of P-gp data in the literature made it possible to select data of high quality obtained under conditions comparable to those used in our studies of BCRP and MRP2 inhibition (see below: "Classification of ABC Transporter Inhibition Data"). The structural diversity of the final dataset was illustrated by the fact that it covered the chemical space of registered oral drugs (Supporting Information, Fig. S1).

The solubility of all compounds included in the data set was predicted using a previously published *in silico* model (47). Compounds predicted to have lower solubility than the concentrations used in this assay were excluded. In addition, all compounds were tested for the formation of reversible aggregates using dynamic light scattering (Zetasizer, Malvern Instruments Limited, Malvern, UK). Compounds that formed aggregates at the same concentration and buffer conditions as used in the inhibition screen were excluded from the analysis unless they: (a) showed specificity towards one or two of the ABC transporters under investigation, or (b) had been reported as transported substrates, since this indicates that the inhibitory effect is competitive and caused by a specific interaction with the transport binding site (48).

Cell Culture Procedure

Saos-2 cells transfected with wild-type (Arg^{482}) human BCRP (Saos-2/wtABCG2) and control cells transfected with the parental transfection vector pcDNA3 (Saos-2/pcDNA3) were kindly provided by Dr. John D. Schuetz of St. Jude Children's Research Hospital, Memphis, TN (49). MDCKII cells transfected with human wild-type P-gp and the untransfected parental cell line were kindly provided by Dr. Piet Borst, Division of Molecular Biology and Center of Biomedical Genetics, The Netherlands Cancer Institute. Cells were cultured in Dulbecco's modified Eagle's medium (Invitrogen, Carlsbad, CA) containing 10% fetal calf serum (FCS, Sigma-Aldrich, St. Louis, MO), under an atmosphere of 5% CO_2 at 37°C. Genetecin (Invitrogen, Carlsbad, CA) was added to the Saos-2 culturing medium to a final concentration of 1 mg/ml.

ABCG2/BCRP Inhibition Data

A recently developed method was used to determine inhibition of mitoxantrone efflux from Saos-2 cells transfected with human wild-type (Arg^{482}) BCRP or pcDNA3 control (36). Briefly, cells were incubated with 1 μM mitoxantrone, with or without the addition of the compound under study at a concentration of 50 μM. Intracellular fluorescence emitted by mitoxantrone was analyzed using flow cytometry (BeckmanCoulter FC500, BeckmanCoulter, Fullerton, CA). Mitoxantrone transport was significantly lower in the control cell line, and all compounds in the dataset had negligible

[1] A recently published structure of mouse P-gp will facilitate more accurate modeling of the binding of both P-gp substrates and inhibitors (Aller et al., Science 2009;323:1718-22. doi:10.1126/science.1168750).

Table I. Inhibitory Effects of the Investigated Compounds on P-gp, BCRP and MRP2

	BCRP	MRP2						
	Mitoxantrone accumulation[a]	Relative transport rate[b]					Molecular weight	Number of
Substance	% inhibition	% inhibition	ABCB1P-gp[c]	ABCG2BCRP[d]	ABCC2MRP2[d]	log$D_{7.4}$	g mol^{-1}	aromatic bonds
Completely overlapping compounds								
Chlorprotixene	78[e]	75	●	●	●	4.3	316	12
Cyclosporine-A[f]	78[e]	60	●	●	●	4.5	1,203	0
Diethylstilbestrol[f]	96[e]	89	●	●	●	4.6	268	12
Dipyridamole	68[e]	58	●	●	●	1.5	505	11
Flupentixol	73[e]	54	●	●	●	3.7	435	12
GF120918	96[e]	61	●	●	●	4.6	564	24
Isradipine	56[e]	54	●	●	●	3.3	371	10
Ivermectin	102	72	●	●	●	5.5	875	0
Loperamide	62[e]	54	●	●	●	4.8	477	18
Lopinavir	66[e]	67	●	●	●	5.2	629	18
MK571	70	91	●	●	●	1.9	515	17
Quercetin	59[e]	60	●	●	●	1.0	302	12
Reserpine	64	63	●	●	●	3.3	609	16
Ritonavir[f]	59[e]	52	●	●	●	4.3	721	22
Saquinavir[f]	67[e]	59	●	●	●	4.6	671	17
Silymarin[f]	52	86	●	●	●	1.5	482	18
Tamoxifen[f]	64[e]	92	●	●	●	5.0	372	18
Terfenadine[f]	51[e]	97	●	●	●	5.9	472	18
Thioridazine	69[e]	101	●	●	●	4.5	371	12
Partially overlapping compounds								
Benzbromarone	133	89	○	●	●	4.0	424	16
Amiodarone	63[e]	34	●	●	○	4.8	645	16
Apigenin	102	6	●	●	○	2.3	270	12
17β-estradiol[f]	58[e]	−23	●	●	○	3.6	272	6
Biochanin A	125	16	●	●	○	2.8	284	12
Chlorpromazine	63[e]	42	●	●	○	3.9	319	12
Chrysin	106[e]	−10	●	●	○	2.8	254	12
Ergocristine[f]	115[e]	40	●	●	○	4.4	610	16
Felodipine[f]	92[e]	14	●	●	○	4.9	384	6
Gefitinib[f]	100[e]	26	●	●	○	4.4	447	17
Genistein	58	−1	●	●	○	2.2	270	12
Glibenclamide	92[e]	−204	●	●	○	2.7	494	12
Imatinib mesylate	100[e]	26	●	●	○	2.5	494	24
Ketoconazole[f]	80[e]	24	●	●	○	4.1	531	17
Ko143	97[e]	27	●	●	○	3.6	470	10
Medroxyprogesterone	63[e]	−11	●	●	○	3.5	344	0
Mifepristone	53[e]	−34	●	●	○	4.9	430	6
Nicardipine	101[e]	41	●	●	○	4.4	480	12
Nitrendipine[f]	75[e]	−124	●	●	○	3.4	360	6
Simvastatin	64[e]	39	●	●	○	4.6	419	0
Tipranavir	92[e]	12	●	●	○	5.0	603	18
Verapamil	71[e]	44	●	●	○	3.7	455	12
Diltiazem	6[e]	60	●	○	●	2.4	415	12
Taurolithocholic acid[f]	−2	73	●	○	●	2.1	484	0
Specific inhibitors								
Haloperidol	2	−6	●	○	○	3.2	376	12
Maprotiline[f]	19[e]	44	●	○	○	2.3	277	12
Noscapine	6	22	●	○	○	1.9	413	12
Prednisone[f]	3[e]	49	●	○	○	1.6	358	0
Procyclidine	1[e]	38	●	○	○	2.6	287	6
Propafenone	13[e]	42	●	○	○	1.6	341	12
Quinidine	0	36	●	○	○	2.4	324	11
Quinine[f]	14[e]	25	●	○	○	2.4	324	11
Taurocholate	0	13	●	○	○	0.1	516	0
Tetracycline	9[e]	−10	●	○	○	−2.6	444	6
Vinblastine	−1	22	●	○	○	4.5	811	16
Amodiaquine[f]	51	40	○	●	○	3.6	356	17

Table I. (continued)

Substance	BCRP: Mitoxantrone accumulation[a] % inhibition	MRP2: Relative transport rate[b] % inhibition	ABCB1P-gp[c]	ABCG2BCRP[d]	ABCC2MRP2[d]	log$D_{7.4}$	Molecular weight g mol^{-1}	Number of aromatic bonds
Fumitremorgin C[f]	77[e]	*n. d.*[g]	○	●	○	2.2	379	10
Hoechst 33342	60[e]	30	○	●	○	3.1	453	26
Mitoxantrone	*n. d.*[h]	−75	○	●	○	−2.6	444	12
Naringenin	57	−107	○	●	○	1.7	272	12
Omeprazole	56[e]	−1	○	●	○	1.6	345	16
Prazosin	68[e]	22	○	●	○	1.6	383	16
Progesterone	56[e]	−23	○	●	○	3.9	314	0
Bromosulfalein	−1	95	○	○	●	0.4	794	18
Lansoprazole	2[e]	66	○	○	●	2.0	369	16
P-aminohippuric acid	0	54	○	○	●	−4.2	194	6
Rifampicin	1	82	○	○	●	1.9	823	11
Compounds without inhibitory effects								
1-methyl-4-phenylpyridinium	1	28	○	○	○	0.5	170	12
4-Methylumbelliferone glucuronide	0	−11	○	○	○	−2.9	352	6
Amantadine[f]	3[e]	−1	○	○	○	−0.4	151	0
Amiloride	1[e]	18	○	○	○	−3.3	230	6
Amitriptyline[f]	0	49	○	○	○	3.1	277	12
Antipyrine	2[e]	16	○	○	○	1.3	188	6
Atropine	0[e]	41	○	○	○	0.8	289	6
Budesonide	7[e]	−50	○	○	○	2.3	431	0
Captopril	0[e]	−4	○	○	○	−2.2	217	0
Carbamazepine	4[e]	14	○	○	○	2.4	236	12
Carnitine	0	16	○	○	○	−3.0	162	0
Cefamandole	−2	37	○	○	○	−3.3	463	11
Chloroquine	−1	−2	○	○	○	2.0	320	11
Chlorzoxazone[f]	2[e]	26	○	○	○	1.8	170	6
Cholic acid[f]	0	−12	○	○	○	1.7	409	0
Cimetidine	1[e]	9	○	○	○	0.2	252	5
Colchicine	−1	−1	○	○	○	1.8	399	6
Dehydroisoandrosterone-3-sulfate	−3	−295	○	○	○	0.3	368	0
Desipramine[f]	−2[e]	43	○	○	○	1.8	266	12
Digoxin	14[e]	1	○	○	○	2.4	781	0
Doxorubicin	*n. d.*[i]	13	○	○	○	0.2	544	12
Erythromycin[f]	6[e]	11	○	○	○	3.1	734	0
Estradiol-17β-glucuronide	4[e]	−8	○	○	○	−0.9	449	6
Etoposide	4[e]	−10	○	○	○	0.3	589	12
Fexofenadine[f]	13[e]	3	○	○	○	2.4	502	18
Flucloxacillin	0	27	○	○	○	−0.5	454	11
Hydrochlorothiazide	4[e]	6	○	○	○	−0.3	298	6
Hydrocortisone[f]	−3[e]	−24	○	○	○	1.6	362	0
Indinavir	3	7	○	○	○	4.6	614	18
Indomethacin[f]	1[e]	−208	○	○	○	0.2	358	16
Mesalazine	−6[e]	−9	○	○	○	−2.0	153	6
Methotrexate[f]	7[e]	−30	○	○	○	−4.8	454	17
Metoprolol[f]	−2[e]	28	○	○	○	0.2	267	6
Nevirapine[f]	7[e]	−21	○	○	○	1.5	266	12
Nicotine	−1	−1	○	○	○	0.2	162	6
Ofloxacin	1	17	○	○	○	−3.0	361	6
Phenobarbital[f]	−1	2	○	○	○	1.4	232	6
Phenylethyl isothiocyanate	5	6	○	○	○	3.7	163	6
Phenytoin[f]	3[e]	−25	○	○	○	2.1	252	12
Pravastatin	−2[e]	−35	○	○	○	0.4	425	0
Prednisolone[f]	1[e]	−10	○	○	○	1.5	360	0
Probenecid	0	−10	○	○	○	−1.0	285	6
Propranolol	0[e]	31	○	○	○	1.2	259	11
Ranitidine[f]	2[e]	48	○	○	○	0.7	314	5

Table I. (continued)

Substance	BCRP: Mitoxantrone accumulation[a] % inhibition	MRP2: Relative transport rate[b] % inhibition	ABCB1P-gp[c]	ABCG2BCRP[d]	ABCC2MRP2[d]	log$D_{7.4}$	Molecular weight g mol^{-1}	Number of aromatic bonds
Sotalol	0[e]	4	○	○	○	−1.5	272	6
Sparfloxacin	1	−38	○	○	○	−2.9	392	6
Sulfasalazine	−8[e]	23	○	○	○	1.3	398	18
Sulfinpyrazone	−3[e]	−50	○	○	○	−1.2	404	18
Sulindac	−1[e]	−51	○	○	○	0.3	356	12
Testosterone[f]	6	−40	○	○	○	3.3	288	0
Tinidazole	13[e]	45	○	○	○	−0.4	247	5
Trimethoprim[f]	3[e]	−7	○	○	○	1.3	290	12
Valproic acid[f]	−1	6	○	○	○	0.3	144	0
Warfarin[f]	2[e]	−36	○	○	○	1.1	308	12
Vincristine	−1	18	○	○	○	4.2	825	16
Zidovudine	−2[e]	−3	○	○	○	−0.2	267	0

[a] Expressed as the ratio of mitoxantrone accumulation after co-incubation with inhibitor to the accumulation observed in Saos-2/wtABCG2 cells incubated with mitoxantrone only. The inhibition ratios were normalized to the value obtained with the potent BCRP inhibitor Ko143 (100% inhibition) to account for inter-day variability. Ko143 and Fumitremorgin C were tested at a concentration of 0.5 μM, GF120918 at 10 μM. All other compounds were tested at a concentration of 50 μM

[b] Expressed as the ratio between ATP-dependent $E_{17}G$ transport rate in MRP2 over-expressing inside-out membrane vesicles in the presence and absence of 80 μM of the test compound. Ko143 was tested at 0.5 μM. The inhibitor concentration was selected to elicit an effect on the transport rate similar to that seen in the BCRP assay, according to Michaelis–Menten kinetics assuming competitive inhibition. Compounds that significantly decreased the ATP-dependent transport rate to less than 50% of the control were regarded as MRP2 inhibitors. The values were taken from Pedersen *et al.* (37)

[c] Classification of the inhibitory effect reported in the literature; ● denotes compounds reported to reduce transport by more than 50% at concentrations comparable to the BCRP and MRP2 assays, or that have reported IC_{50} values below 50 μM. ○ denotes compounds with reported negative results in inhibition assays comparable to the BCRP and MRP2 assays

[d] Classification of the experimentally determined BCRP and MRP2 inhibition. ● denotes inhibitors, ○ denotes non-inhibitors

[e] Values from Matsson *et al.* (36)

[f] Test set compounds

[g] Value from Rabindran *et al.* (46)

[h] Value from Volk *et al.* and Suzuki *et al.* (44,45)

[i] Value from Suzuki *et al.* (45)

intrinsic fluorescence at the selected wavelength (data not shown). The increase in intracellular accumulation of mitoxantrone on co-incubation with the compounds under study was used as a measure of BCRP inhibition and was normalized to that obtained using 0.5 μM of the potent BCRP inhibitor Ko143 (100% inhibition). BCRP inhibition was determined for 41 compounds in this study as was the concentration dependent inhibition by GF120918, Ko143, MK571, chlorprothixene, loperamide, thioridazine, haloperidol, prazosin and bromosulfalein. The dataset was complemented with data for 81 compounds from Matsson *et al.* (36), obtained using the same method as above (Table I).

ABCC2/MRP2 Inhibition Data

Inhibition data for MRP2-mediated estradiol-17-β-D-glucuronide ($E_{17}G$) transport were taken from Pedersen *et al.* (37). Briefly, 10 μg inverted Sf9 membrane vesicles over-expressing human MRP2 (Solvo Biotechnology, Budapest, Hungary) were incubated with 50 μM $E_{17}G$ with or without the addition of 80 μM of the compound under study. Intravesicular amounts of radiolabeled $E_{17}G$ were measured in a 1900CA Tricarb liquid scintillation counter (Canberra Packard Instruments, Downers Grove, IL). ATP-dependent transport rates were calculated by subtracting the transport in vesicles incubated with AMP from the rate in ATP-incubated vesicles. The inhibitory effects of the test compounds were calculated as the ratio between the ATP-dependent $E_{17}G$ transport rate in the presence and absence of the test compound. The same method was used to determine the concentration-dependent inhibitory effects of GF120918, Ko143, MK571, chlorprothixene, loperamide, thioridazine, haloperidol, prazosin and bromosulfalein in this study.

ABCB1/P-gp Inhibition Data

Data for drug-mediated inhibition of P-gp were collected from a large number of sources in the literature through a search of the transporter database available from the University of Tokyo (50), as well as through searches conducted in the PubMed literature database (http://www.ncbi.nlm.nih.gov/sites/entrez) using the keywords P-gp, P-glycoprotein, MDR-1 and ABCB1. Only studies using cell lines or membrane vesicles from cell lines over-expressing human P-gp were included in the analysis to ensure that the inhibition was related to P-gp and that it was not biased by other transporters. The concentration-dependent inhibitory effects of GF120918, Ko143, MK571, chlorprothixene, loperamide,

thioridazine, haloperidol, prazosin and bromosulfalein were determined as described previously (51,52). Briefly, MDCKII cells transfected with human P-gp were incubated with 1 μM calcein-AM, with or without the addition of the compound under study. The intracellular accumulation of calcein was determined fluorometrically using a Tecan Saphire^2 plate reader (Tecan, Männedorf, Switzerland). Initial appearance rates were determined from the linear part of the fluorescence-time plot (0–30 min after addition of calcein-AM). The increase in the intracellular accumulation of calcein on co-incubation with the compounds under study was used as a measure of P-gp inhibition and was normalized to the value obtained using 1 μM of the potent P-gp inhibitor GF120918 (100% inhibition).

Classification of ABC Transporter Inhibition Data

To enable unbiased comparisons to be made between P-gp, BCRP and MRP2, the same criteria for identification of inhibitors were used for all three transporters. Compounds were regarded as inhibitors if they reduced transport by at least 50%, using inhibitor concentrations in the vicinity of the K_m-values for each transporter's probe substrate. The inhibitor concentrations used in the screen were selected to pick up both high-affinity inhibitors and compounds with intermediate transporter affinity, since concomitant administration of multiple inhibitors of this type has been shown to have additive effects on drug disposition (53).

For BCRP, an inhibitor concentration of 50 μM was used, which corresponds to approximately 2.5× the K_m (18±3 μM) observed for the mitoxantrone transport in Saos-2 cells over-expressing BCRP (36). For MRP2, an inhibitor concentration of 80 μM was selected, close to the K_m (94±7 μM) observed for the MRP2-mediated transport of $E_{17}G$ in Sf9 membrane vesicles (37) (Table II). For P-gp, compounds were classified as inhibitors if transport was reduced by at least 50% at an inhibitor concentration of ≤50 μM. To facilitate comparisons with our experimental results for BCRP and MRP2, the inhibitor concentration was chosen within the same concentration range as that of the reported K_m-values for the P-gp substrates used, typically ranging from 10 to 20 μM (11,54,55) (Table II). In line with the selected cutoff, compounds were noted as being P-gp inhibitors if: (a) concentration-dependent inhibition studies had demonstrated that the IC_{50} or K_i values were lower than 50 μM, or (b) single-point determinations had shown at least 50% inhibition of P-gp-mediated transport at a concentration not exceeding 50 μM.

Computational Modeling

Molecular structures obtained from SciFinder Scholar 2006 (American Chemical Society, Washington DC) were used as the input for 3D structure generation using Corina version 3.0 (Molecular Networks, Erlangen, Germany). A total of 669 molecular descriptors, representing mainly molecular size, flexibility, connectivity, polarity, charge, and hydrogen bonding potential, were calculated from the 3D structures using DragonX version 3.0 (Talete, Milan, Italy), ADMETPredictor version 1.2.4 (SimulationsPlus, Lancaster, CA), and HYBOT (MOLPRO-2001, TimTec, Newark, DE). The static free molecular surface areas for each different atom type were calculated using the in-house software MAREA version 3.02, as described previously (56,57). After removal of replicate molecular descriptors and descriptors having zero variance, 240 descriptors remained and were used as a starting point for the model development.

Partial least-squares projection to latent structures discriminant analysis (PLS-DA), as implemented in Simca-P version 11.5 (Umetrics, Umeå, Sweden), was used to derive multivariate classification models for separating inhibitors from non-inhibitors or to separate specific inhibitors for different transporters from each other (Fig. 4). The computational models were developed in four steps. First, each of the three transporters were investigated separately (Fig. 4A), and important molecular characteristics for the inhibition of each of them were revealed. Secondly, a model describing inhibition of ABC transporters in general was developed (Fig. 4B). The results from this model were compared with those obtained by combining the predictions from the individual models (Fig. 4C; Results in Supplementary Material). Finally, the specific inhibitors of P-gp and BCRP were modeled in order to reveal molecular features responsible for specific binding to these two transporters (Fig. 4D). In this step, MRP2 was excluded due to the low number of specific inhibitors identified for this transporter (n=4).

The influence of differently sized groups on the models was balanced by replication of the compounds belonging to the smaller classes in the datasets. To avoid bias in the models, all replicates of a molecule were removed simultaneously during the cross-validation procedure. The models

Table II. Selection of Comparable Inhibitor Concentrations for Assays of BCRP, MRP2 and P-gp Inhibition

	K_m	Substrate concentration	K_i	Inhibitor concentration	Relative transport rate[a]
	μM	μM	μM	μM	%
P-gp	10	1	50	50	52
(examples)	20	2	50	50	52
BCRP	18[b]	1	50	50	51
MRP2	94[c]	50	50	80	49

Suitable inhibitor concentrations were selected based on kinetic parameters, so that the effect of the inhibitors on the transport rate would be similar for all transporters.
[a] Assuming competitive Michaelis–Menten kinetics
[b] Determined by Matsson *et al.* (36)
[c] Determined by Pedersen *et al.* (37)

were optimized by a variable selection procedure in which groups of molecular descriptors that did not contain information relevant to the problem (*i.e.*, noise) were removed in a stepwise manner. Descriptors were excluded from the model if their removal resulted in a statistically improved model, based on the classification accuracy for the training set. The statistical validity of the models was tested using a random permutation test, in which the order of the response variable was randomly changed 100 times. All presented models collapsed to sub-zero cross-validated coefficients of determination (Q^2) when the response variables were permutated, demonstrating that the models do not describe noise, but are indeed describing the response variables. In addition, the external predictive powers of the models were determined using a test set of 39 compounds that were withheld from the model development. The test set was randomly selected so that it contained one-third of the total number of compounds in each of the following groups: (a) P-gp inhibitors, (b) P-gp non-inhibitors, (c) BCRP inhibitors, (d) BCRP non-inhibitors, (e) MRP2 inhibitors, and (f) MRP2 non-inhibitors. Compounds that increased MRP2-mediated transport rates were excluded from the MRP2 model, in order to limit the bias from stimulatory binding. The same training and test set division was used for all developed models, except for the model of specific inhibitors, because of the small sizes of the specific inhibitor subsets.

Virtual Docking of Inhibitors

Three-dimensional molecular structures of multi-specific ABC transporter inhibitors (obtained as described above) were imported into Maestro version 8.5 (Schrödinger, San Diego, CA). The crystal structure of the conserved human MRP1 (ABCC1) nucleotide binding domain 1 (Protein Data Bank ID 2CBZ) was used as the template for the docking. The protein and ligands were prepared using default settings of the Maestro protein and ligand preparation procedures, respectively. The ligands were docked using Glide XP version 5.027 (Schrödinger, San Diego, CA) and default docking parameters. The alignments of ATP and the docked inhibitors were visualized using Accelrys DS Visualizer version 2.0.1 (Accelrys, San Diego, CA), and QuteMol version 0.4.1 (58).

RESULTS

Overlapping Inhibitor Spaces for ABC Transporters

The inhibitor specificities of P-gp, BCRP and MRP2 are shown in Fig. 1 and Table I. Of the 122 tested compounds, 66 (54%) inhibited at least one of the transporters under comparable assay conditions. The number of inhibitors was almost twice as high for P-gp and BCRP, with 53 (43%) and 49 (40%) inhibitors, respectively, as for MRP2, which was inhibited by a total of 26 compounds (21%). General ABC transporter inhibitors, exhibiting completely overlapping affinity, made up the majority (73%) of the MRP2 inhibitors and also contributed significantly to the inhibitor space for P-gp (36%) and BCRP (39%). In comparison, 21%, 16% and 15% of the P-gp, BCRP and MRP2 inhibitors, respectively, were specific for that transporter.

The greatest similarity in the affinity patterns was observed for P-gp and BCRP, with 40 inhibitors being

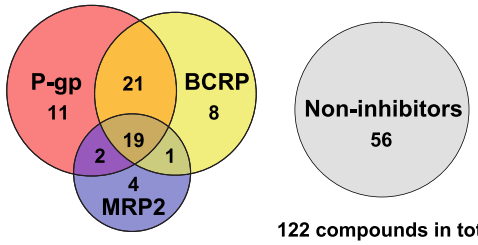

Fig. 1. Overlapping inhibition of the major efflux transporters, P-gp (ABCB1), BCRP (ABCG2) and MRP2 (ABCC2). In total, 66 (54%) of the compounds inhibited one or more of the transporters studied. The number of specific inhibitors were 11, 8 and 4 for P-gp, BCRP and MRP2, respectively. A large overlap was observed between P-gp and BCRP, with 40 inhibitors in common.

common to both transporters, 21 of which did not significantly inhibit MRP2-mediated transport at the screening concentration. In contrast, only one inhibitor (benzbromarone) was shared by MRP2 and BCRP while not affecting P-gp (Table I). Similarly, only diltiazem and taurolithocholic acid inhibited P-gp and MRP2 while not affecting BCRP (Table I). Our results corroborate previous indications that there is a significant overlap in affinity between the major drug efflux transporters P-gp, BCRP and MRP2 (1,2,59,60), with almost two-thirds of the inhibitors in our study affecting more than one transporter.

It is noteworthy that MK571, which is commonly used as a MRP specific inhibitor (61), was shown to inhibit all three of the ABC-transporters under the selected assay conditions. Similarly, GF120918 and Ko143, which are often used as specific inhibitors of P-gp/BCRP and BCRP, were both shown to have wider inhibition specificities than expected: GF120918 inhibited all three transporters at the selected screening concentration, and Ko143 inhibited both BCRP and MRP2. To follow up these results, the inhibitory concentration range was examined in greater detail for these three compounds (Fig. 2A–C).

In agreement with the screening results, MK571 was shown to inhibit all three transporters with IC_{50} values of the same order of magnitude (10, 26 and 50 μM for MRP2, P-gp and BCRP, respectively); limiting its use as an MRP-specific inhibitor, but suggesting its use as a general inhibitor of ABC transport proteins. Preliminary results from three alternative experimental systems (inverted HEK293 membrane vesicles over-expressing each of the ABC-transporters investigated), confirmed that the overlapping affinity was not an artifact of the particular experimental models used here (unpublished results, Pedersen *et al.*, 2009). GF120918 was also shown to inhibit all three transporters, but with IC_{50} values spanning three log units (Fig. 2A). The results suggest that GF120918 is specific for P-gp in a concentration range between 300 nM and 5 μM, with an optimal specificity at 1 μM where 87% of the P-gp transport was inhibited. Combined P-gp and BCRP inhibition was observed at concentrations above 20 μM, with only limited affinity for MRP2 up to 100 μM. Correspondingly, Ko143 specifically inhibited BCRP at concentrations between 200 nM and 1 μM and inhibited MRP2 at low micromolar concentrations, but had markedly lower affinity for P-gp ($IC_{50} \gg 10$ μM). Thus, for the high-affinity inhibitors GF120918 and Ko143, the screening concentration used in this study was outside the range of optimal selectivity. To

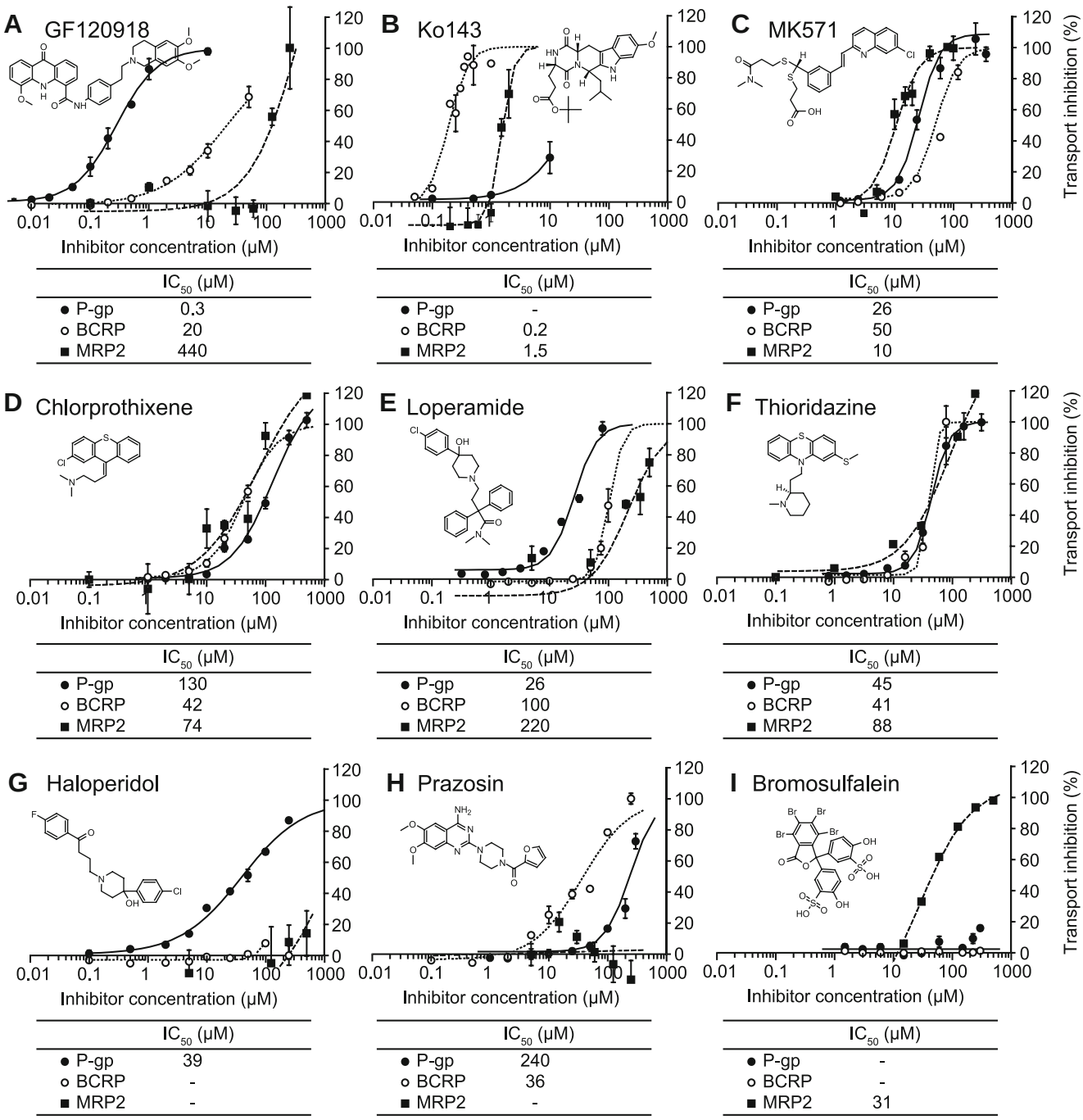

Fig. 2. Concentration dependent inhibitory effect of GF120918 (**A**), Ko143 (**B**), MK571 (**C**), chlorprothixene (**D**), loperamide (**E**), thioridazine (**F**), haloperidol (**G**), prazosin (**H**) and bromosulfalein (**I**), on P-gp, BCRP and MRP2 transport. IC_{50} values, defined as the concentration resulting in half-maximum inhibition, were determined using non-linear regression. In particular, MK571 was shown to have comparable affinity for all three of the transporters studied, with the IC_{50} values being within one log unit of one another (**C**). GF120918 and Ko143 showed preferential affinity towards P-gp/BCRP and BCRP, although affecting MRP2 at higher concentrations (**A** and **B**). Three of the specific inhibitors identified in this study showed selective affinity for P-gp (haloperidol), MRP2 (bromosulfalein) and BCRP/P-gp (prazosin) within a broad concentration range (**G**–**I**), whereas similar affinity for all three transporters was confirmed for the three multi-specific inhibitors (**D**–**F**). For MRP2, some of the tested compounds stimulated substrate transport at low concentrations, resulting in negative inhibition values.

investigate if similar off-target effects were underlying the relatively large number of compounds inhibiting all three transporters, we selected three multi-specific inhibitors from our screen (chlorprothixene, loperamide and thioridazine) for concentration dependency studies. Corroborating the screening results, all three compounds exhibited similar affinities for P-gp, BCRP and MRP2, with IC_{50} values for all transporters within a 0.3, 0.5 and 0.9 log unit range for thioridazine, chlorprothixene and loperamide, respectively (Fig. 2D–F).

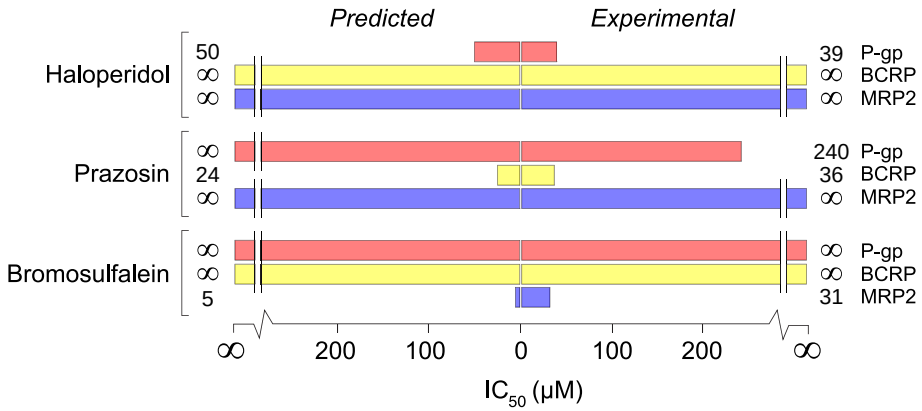

Fig. 3. The correspondence between IC_{50} values predicted from single-concentration data (*left-hand side*) as explained in the Results section "Overlapping Inhibitor Spaces for ABC Transporters" and footnote 1 and experimentally determined values (*right-hand side*). *Red bars* show the experimental and predicted IC_{50} values for inhibition of P-gp; *yellow bars* show the IC_{50} values for BCRP inhibition; and *blue bars* show the IC_{50} values for MRP2 inhibition. In general, the predicted IC_{50} values agreed well with the values determined experimentally.

In contrast to the multi-specific inhibitors, compounds that were specific for a certain transporter at the chosen screening concentration are likely still specific at lower concentrations. To confirm this notion, we also determined the concentration-dependent inhibitory effects of three compounds that showed high selectivity for a single transporter in the screen (haloperidol, prazosin and bromosulfalein; Fig. 2G–I). Predicted IC_{50} values for each transporter's specific inhibitor, assuming classical one-site competition[2], were in good correlation with the experimentally determined values (Fig. 3). This indicates that several other inhibitors found to be specific at the screening concentration will remain specific at lower concentrations (Table I). The results from the IC_{50} determinations suggest that bromosulfalein is more suitable than MK571 as an MRP specific inhibitor and that haloperidol and prazosin can be used as alternatives for specific P-gp and BCRP inhibition, although they have lower affinities than GF120918 and Ko143.

Structural Characteristics of ABC Transporter Inhibitors

Computational models developed for each one of the three transporters revealed a comparable importance of lipophilicity, aromaticity and size for transporter inhibition (Figs. 4A and 5A–C). A similar result was observed in a model discriminating inhibitors of any of the three ABC transporters from compounds defined as non-inhibitors (Figs. 4B and 5D; Fig. S2). It is apparent that lipophilicity and aromaticity are important characteristics of the ABC transporter inhibitors in this dataset. To further investigate whether high lipophilicity and aromaticity are common characteristics of ABC transporter inhibitors, we analyzed

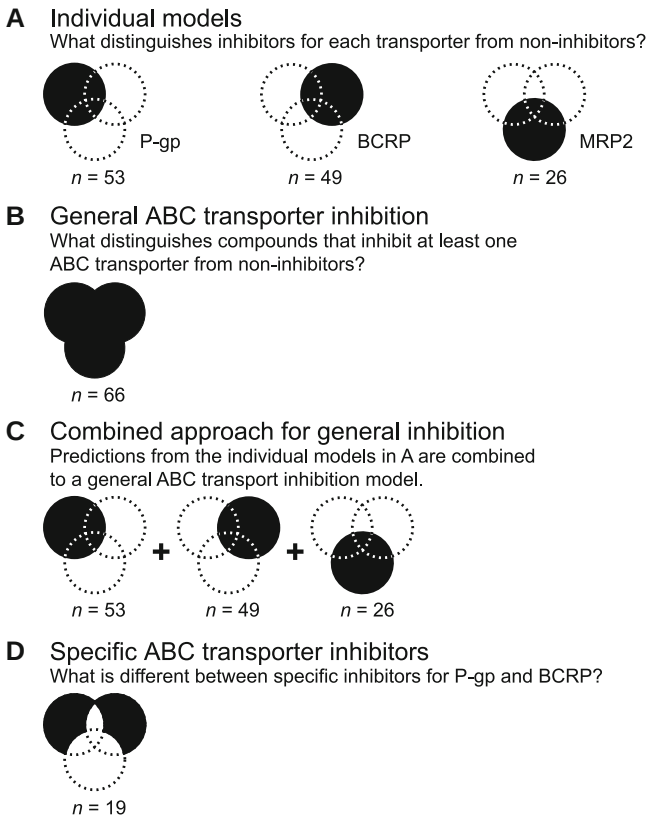

Fig. 4. Approaches for modeling ABC transport inhibitors. Computational models were developed for different subsets of the compounds in this study. **A** Individual models for P-gp, BCRP and MRP2; **B** model of compounds inhibiting any of the three ABC transporters; **C** an alternative approach for modeling general ABC transporter inhibition, by combining the predictions from the individual models developed in **A**; **D** model of specific inhibitors for P-gp and BCRP. The same order of the *circles* is used throughout the paper, with P-gp in the *top left*, BCRP in the *top right*, and MRP2 in the *bottom*.

[2] The approximate concentration range was calculated assuming a sigmoidal concentration dependency of the inhibitory effect: $\%transport = 100/1 + 10^{(I-IC50)\gamma}$, where I is the inhibitor concentration, IC_{50} is the inhibitor concentration resulting in a 50% reduction of the transport rate, and γ is the slope of the curve. Assuming a slope of 1, as generally observed for concentration-dependent transport inhibition, a compound resulting in a 10% reduction of the transport rate at a concentration C will inhibit the transport by 50% at a concentration $9\times C$. If the sigmoidal relationship has a steeper slope of, say, 3, the compound will give 50% inhibition at a concentration $2.1\times C$.

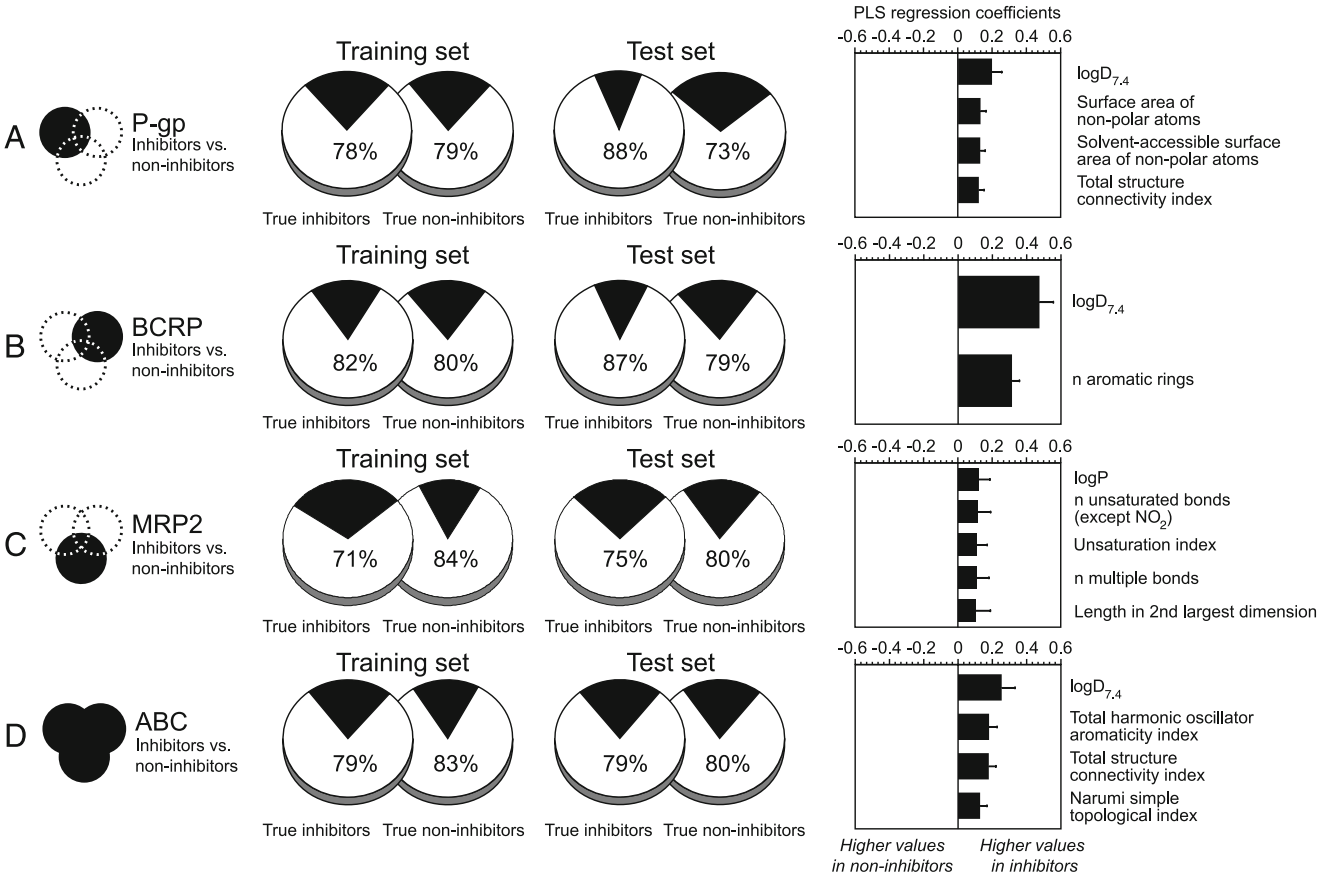

Fig. 5. Prediction of ABC transporter inhibitors from individual models for P-gp (**A**), BCRP (**B**), and MRP2 (**C**), and from a model of general ABC transporter inhibition (**D**). The *pie charts* show the percentage of correct classifications for the inhibitors in the training set, the non-inhibitors in the training set, the inhibitors in the test set, and the non-inhibitors in the test set (*from left to right*). *White* denotes correct classifications and *black* denotes false ones. The *right-hand plots* show PLS regression coefficients for the molecular descriptors included in the final models after step-wise exclusion of insignificant descriptors, as described in the "MATERIALS AND METHODS" section. The molecular descriptors are related to the lipophilicity (log*P*, log$D_{7.4}$, and the surface area of non-polar atoms), size and shape (length in the second largest dimension, total structure connectivity index, and the Narumi simple topological index) and aromaticity (number of aromatic rings, number of unsaturated/multiple bonds, unsaturation index, and total harmonic oscillator aromaticity index). Descriptors with large absolute coefficients have a large influence on the discriminant model. Positive coefficients mean that the inhibitors have higher descriptor values, whereas descriptors with negative coefficients have higher values in non-inhibitors. The *symbols in the column furthest to the left* describe the compounds included in the model, with P-gp as the *top left circle*, BCRP as the *top right one*, and MRP2 as the *circle at the bottom*.

the distribution of these properties in the different subgroups of the dataset (Fig. 6; Table III). The compounds in the complete dataset had values of log$D_{7.4}$ ranging from −4.8 to 5.9. The average lipophilicity of the ABC transporter inhibitors was higher than for the non-inhibitors, although the extremes in both groups make the span from the lowest to the highest value comparable. The multi-specific inhibitors exhibited a tighter lipophilicity distribution that was shifted to higher values (≥1.0) than that of the specific inhibitors ($p<0.05$). The median log$D_{7.4}$ was 2.3, 1.9 and 1.2 for the specific P-gp, BCRP, and MRP2 inhibitors, respectively, whereas the multi-specific inhibitors had a median log$D_{7.4}$ of 4.5 (Fig. 6A; Table III). Correspondingly, the number of aromatic bonds was generally higher in the inhibitor groups than in the non-inhibitors (Table I; Supporting Information, Fig. S3A; $p<0.01$). With the exception of the specific P-gp inhibitors, which usually had 6–12 aromatic bonds, the inter-quartile range was similar in both the overlapping and the specific inhibitors, with most inhibitors containing 12–18 aromatic bonds.

Virtual Docking of Multi-Specific Inhibitors to the ATP-Binding Domain

Since the major part of the sequence similarity between different ABC transporter superfamily members is found in the ATP-binding domain (25,31), we hypothesized that inhibitor competition with ATP binding might be underlying the marked affinity overlap in this study. Multi-specific inhibitors were docked to a high resolution crystal structure of the conserved ATP-binding domain of MRP1 (63) to determine whether this was the case. The native ligand ATP docked with high scores in the same orientation as that observed in the crystal structure. The docked structure of MK571, which differs from most other multi-specific inhibitors by being less lipophilic and by carrying a negative charge at physiological pH, interacted with the same amino acids in the catalytic site as ATP (Fig. 7A–C). This suggests that, in addition to the competitive inhibition at the transporter site reported for MRPs (64), competition with ATP binding could

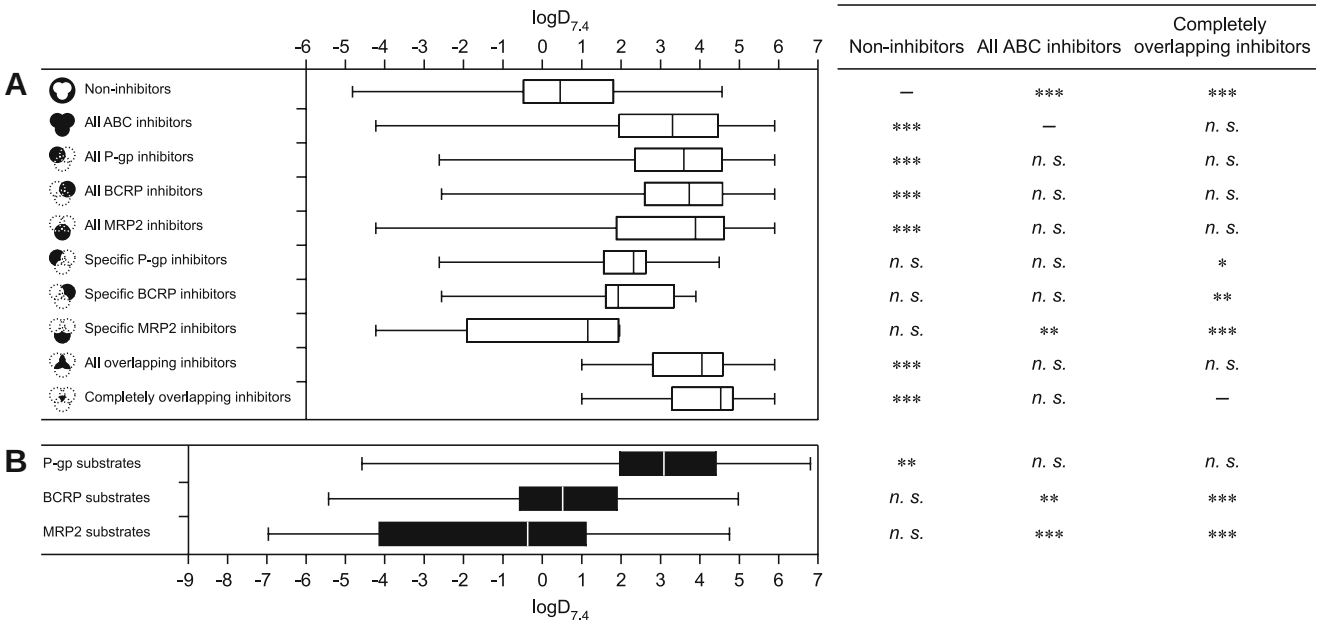

	Non-inhibitors	All ABC inhibitors	Completely overlapping inhibitors
Non-inhibitors	–	***	***
All ABC inhibitors	***	–	*n. s.*
All P-gp inhibitors	***	*n. s.*	*n. s.*
All BCRP inhibitors	***	*n. s.*	*n. s.*
All MRP2 inhibitors	***	*n. s.*	*n. s.*
Specific P-gp inhibitors	*n. s.*	*n. s.*	*
Specific BCRP inhibitors	*n. s.*	*n. s.*	**
Specific MRP2 inhibitors	*n. s.*	**	***
All overlapping inhibitors	***	*n. s.*	*n. s.*
Completely overlapping inhibitors	***	*n. s.*	–
P-gp substrates	**	*n. s.*	*n. s.*
BCRP substrates	*n. s.*	**	***
MRP2 substrates	*n. s.*	***	***

Fig. 6. Lipophilicity of the compounds in this study. **A** Distribution of log$D_{7.4}$ in the subgroups of the dataset. **B** Distribution of log$D_{7.4}$ in substrates of P-gp, BCRP and MRP2 (50,62). The *boxes* show the inter-quartile distances and the median values, and the *whiskers* show the span between the lowest and the highest value. The overlapping inhibitors have a higher lipophilicity than the specific inhibitors. The *symbols to the left* describe the compounds included in each subset, with P-gp as the *top left circle*, BCRP as the *top right one*, and MRP2 as the *circle at the bottom*. Anova with Tukey's post test was used to test the significance of the inter-group differences, with *one*, *two* and *three stars* denoting $p<0.05$, $p<0.01$, and $p<0.001$, respectively. *n.s.*: not significant ($p>0.05$).

be contributing to the surprisingly broad specificity of MK571. The two most hydrophilic multi-specific inhibitors, quercetin and silymarin, also docked with high scores to the catalytic site, which is in line with previous results (65,66). In contrast, the prototypical lipophilic inhibitors chlorprothixene, loperamide and thioridazine (log$D$=4.3, 4.8 and 4.5, respectively; Fig. 2D–F) did not interact with the catalytic site (Fig. 7D) and had low docking scores, comparable to those of a selection of non-inhibitors (data not shown). This indicates that the lipophilic multi-specific inhibitors rather interact with a site distinct from the ATP-binding domain.

Specific Inhibitors of P-gp and BCRP

Although the majority of the compounds inhibiting P-gp and BCRP were common to both transporters, differences in the affinity pattern apparently exist, resulting in 11 inhibitors specific for P-gp and eight for BCRP in this study. A multivariate analysis of the molecular descriptors defining this difference (Fig. 4D) showed that for this limited set of 19 compounds, the BCRP inhibitors contained a larger number of nitrogen atoms, in particular aromatic nitrogens, than did the P-gp inhibitors (Fig. 8). Furthermore, the multivariate

Table III. Physicochemical Properties of the Subgroups in the Dataset

		log$D_{7.4}$[a]			Total structure connectivity index[b]			Number of aromatic bonds[c]		
	n	Mean±SE	Median	Range	Mean±SE	Median	Range	Mean±SE	Median	Range
Non-inhibitors	56	0.5±0.3	0.5	(−4.8–4.6)	0.27±0.009	0.25	(0.15–0.45)	7.4±0.8	6	(0–18)
All ABC transporter inhibitors	66	3.0±0.2	3.3	(−4.2–5.9)	0.22±0.004	0.22	(0.14–0.34)	12.0±0.8	12	(0–26)
All P-gp inhibitors	53	3.3±0.2	3.6	(−2.6–5.9)	0.22±0.004	0.22	(0.14–0.27)	11.6±0.9	12	(0–24)
All BCRP inhibitors	49	3.5±0.2	3.7	(−2.6–5.9)	0.22±0.005	0.22	(0.14–0.27)	12.9±0.9	12	(0–26)
All MRP2 inhibitors	26	3.2±0.4	3.9	(−4.2–5.9)	0.21±0.009	0.21	(0.14–0.34)	13.3±1.2	14	(0–24)
Specific P-gp inhibitors	11	1.8±0.6	2.3	(−2.6–4.5)	0.22±0.008	0.23	(0.15–0.25)	8.9±1.6	11	(0–16)
Specific BCRP inhibitors	8	1.9±0.7	1.9	(−2.6–3.9)	0.23±0.008	0.23	(0.19–0.26)	13.6±2.6	14	(0–26)
Specific MRP2 inhibitors	4	0.0±1.5	1.2	(−4.2–2.0)	0.24±0.04	0.23	(0.16–0.34)	12.8±2.7	14	(6–18)
All overlapping inhibitors	43	3.7±0.2	4.0	(1.0–5.9)	0.22±0.005	0.21	(0.14–0.27)	12.4±1.0	12	(0–24)
Completely overlapping inhibitors	19	3.9±0.3	4.5	(1.0–5.9)	0.20±0.008	0.20	(0.14–0.27)	14.0±1.4	16	(0–24)

[a] Comparative statistics are presented in Fig. 6A
[b] Comparative statistics are presented in the Supporting Information, Fig. S3A
[c] Comparative statistics are presented in the Supporting Information, Fig. S3B

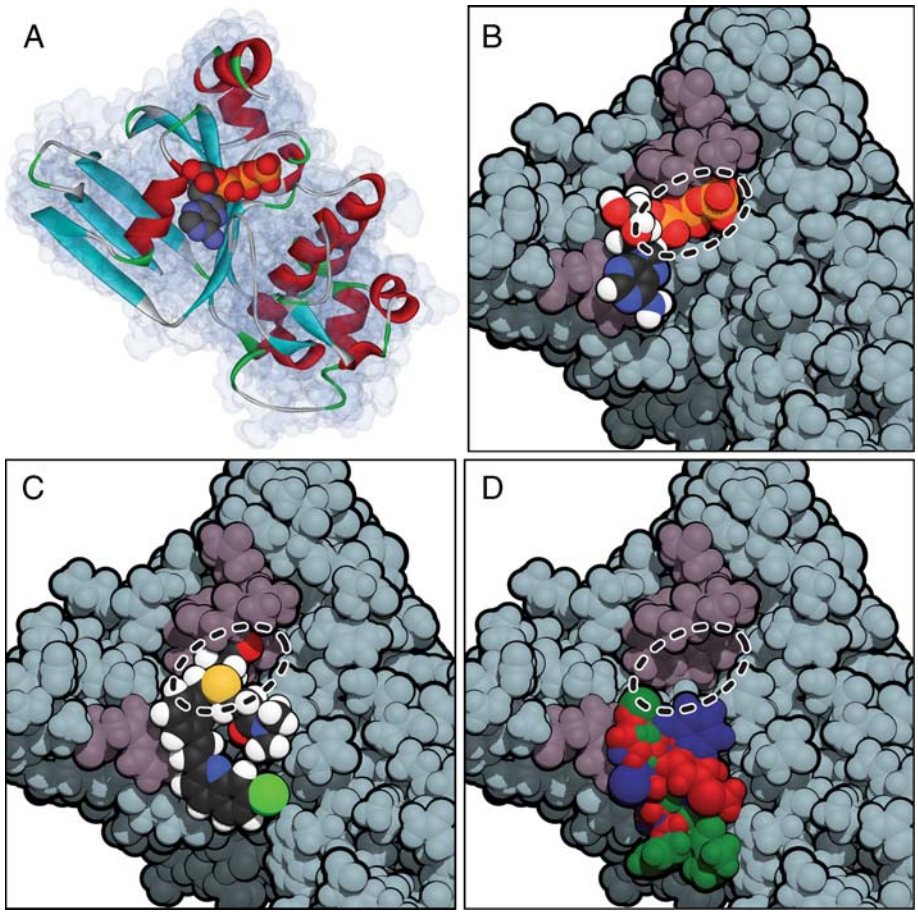

Fig. 7. Virtual docking of multi-specific inhibitors to the ATP-binding site. The crystal structure of the conserved nucleotide binding domain 1 of human MRP1 (ABCC1) was used as the docking template (63). **A**, **B** Ribbon and space-filling representations of the MRP1 ATP-binding domain co-crystallized with ATP. In **B**, Trp653 and the conserved residues of the Walker A motif that are involved in ATP binding and hydrolysis are *highlighted in purple*. The catalytic pocket is *encircled with a dashed line*. **C** Orientation of the negatively charged multi-specific inhibitor MK571 docked to the ATP binding site. The carboxylic acid moiety of MK571 is in close proximity to the residues of the catalytic site, and, analogous to the adenosine base ring in ATP, the conjugated ring interacts with Trp653 through π–π stacking. **D** In contrast to MK571, the lipophilic and basic multi-specific inhibitors chlorprothixene (*blue*), loperamide (*red*) and thioridazine (*green*) do not overlap with the catalytic site.

analysis confirmed the observation that the specific P-gp inhibitors in this study were less aromatic than the rest of the inhibitors. As only four inhibitors in our dataset were specific for MRP2, this subset was not included in the modeling of specific inhibitors.

DISCUSSION

In this paper, the inhibition patterns of the three major human ABC transporters P-gp, BCRP and MRP2 were studied using a dataset of 122 structurally diverse drugs. In total, 66 compounds inhibited at least one of the transporters, and as many as 43 (65%) of these inhibitors affected more than one transporter at the concentration investigated. These results demonstrate, for the first time using a large dataset common to all three transporters, the considerable inhibitor overlap between P-gp, BCRP and MRP2.

Twenty-three compounds were identified as inhibiting only one of the ABC transporters studied at the selected concentration. The results from the screen suggested that haloperidol would specifically inhibit P-gp, with very limited effects on BCRP and MRP2 in an approximate concentration range of up to ten times the standard inhibitor concentration, assuming classical one-site competition (see footnote 1). Correspondingly, it was predicted that prazosin and bromosulfalein would be specific inhibitors of BCRP and MRP2, respectively. The predicted specificity was confirmed for all three compounds in concentration dependent experiments (Fig. 2G–H), and the projected IC_{50} values (see footnote 1) correlated well with the experimentally determined ones (Fig. 3). This indicates that inhibitors that are selective at the screening concentration will also be selective at lower concentrations.

Care was taken to select inhibitor concentrations resulting in relevant and comparable results for P-gp, MRP2 and BCRP to facilitate the development of computational models and enable unbiased comparisons to be made between the transporter's inhibitor patterns. (Table II). However, for

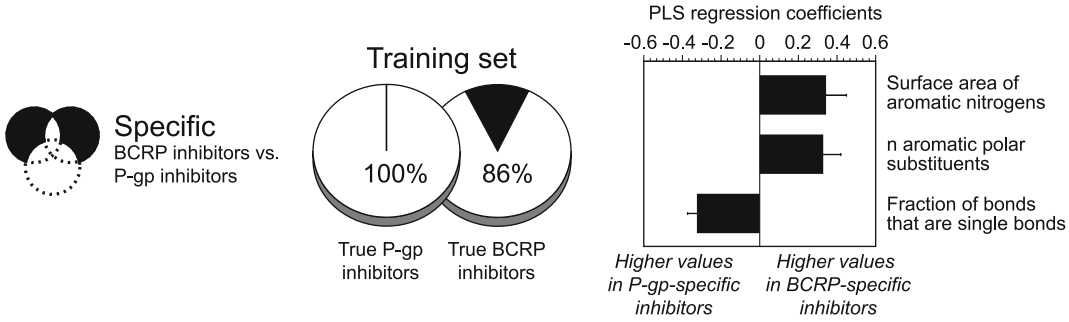

Fig. 8. Prediction of inhibitor specificity. The model was developed to discriminate inhibitors specific for P-gp from BCRP-specific inhibitors. Because of the low number of MRP2-specific inhibitors, this subset was not included in the model. The *pie charts* show the percentage of correct classifications for the inhibitors and non-inhibitors in the training set (*from left to right*). *White* denotes correct classifications and *black* denotes false ones. Because of the small datasets of specific inhibitors, a purely descriptive model was developed, using all compounds for the training set. The *right-hand plots* show PLS regression coefficients for the molecular descriptors included in the final models after step-wise exclusion of insignificant descriptors, as described in the "MATERIALS AND METHODS" section. The molecular descriptors are related to hydrogen bonding (the number of aromatic polar substituents and the surface area of aromatic nitrogens) and aromaticity/lack of aromaticity (the fraction of bonds that are single bonds). Descriptors with large absolute coefficients have a large influence on the discriminant model. Positive coefficients mean that the descriptors have higher values in BCRP inhibitors, whereas descriptors with negative coefficients have higher values in P-gp inhibitors. The *symbols in the column furthest to the left* show which part of the data set was included in the model, with P-gp, BCRP and MRP2 as the *top left*, *top right* and *bottom circles*, respectively.

some inhibitors previously reported as being specific, including GF120918, MK571 and Ko143, the selected concentrations were outside the range of optimal selectivity. These inhibitors have been reported to have higher affinity for P-gp and BCRP (GF120918), for MRPs (MK571) and for BCRP (Ko143) (61,67,68), but were found to inhibit additional ABC transporters under the conditions used in our screening study. The surprisingly broad specificity of these inhibitors was, therefore, followed up by measurements of the concentration-dependent inhibition of P-gp, BCRP and MRP2 for each of the inhibitors. Notably, MK571 was shown to have a comparable affinity for all three of the transporters studied (Fig. 2C), abolishing its utility as an MRP-specific inhibitor. In line with previous reports, GF120918 showed preferential affinity towards P-gp and BCRP (68), and Ko143 towards BCRP (67) although our results demonstrate that the concentrations must be carefully selected to ensure selective inhibition of the transporter of interest (Fig. 2A, B).

In addition to the large affinity overlap that we demonstrate here for three major ABC efflux transporters, shared affinity between efflux transporters and uptake transporters from the solute carrier (SLC) family is a complicating factor in delineating transport in complex systems (69,70). For instance, 12 of the 23 specific inhibitors in our screen have also been listed in the University of Tokyo transporter database as either substrates or inhibitors of SLC transporters (50). Of the inhibitors studied in further detail (haloperidol, prazosin, bromosulfalein, GF120918, Ko143 and MK571), the basic drugs haloperidol and prazosin have been reported to interact with members of the organic cation transporter family (OCT; SLC22A1-3), while the negatively charged bromosulfalein has been identified as a high-affinity substrate for organic anion transporters, including OATP1B1 and OATP1B3 (SLCO1B1/3) and several members of the OAT family (SLC21A6-8) (50,71,72). Although such an overlap may well exist also for GF120918, Ko143 and MK571, we were unable to find any reports in the public domain where the interaction of these compounds with uptake transporters had been studied and, at present, further studies are needed to assure the specificity of these inhibitors. Overlapping affinity for uptake and efflux transporters may limit the utility of these compounds as specific probes for ABC-transport inhibition in complex models expressing functional uptake and efflux transporters (69,73). However, they will be valuable tools for differentiation between efflux transporters in better defined *in vitro* expression systems; for example, the combined specificity of bromosulfalein for OATP1B1/3 and MRP2 would make it an excellent control inhibitor in cell models of hepatobiliary transport (74).

A general physicochemical characteristic of the multi-specific inhibitors in this investigation was their high lipophilicity (median log$D_{7.4}$=4.5; Fig. 6A). According to the prevailing two-step model of drug interaction with P-gp (30,35), the ligands partition into the plasma membrane before binding to the transporter. This explains the reported importance of lipophilicity for P-gp substrates and inhibitors (75). We recently proposed a similar binding mechanism for BCRP inhibitors (36), as well as for a subset of lipophilic inhibitors of MRP2 (37). The notable lipophilicity of the multi-specific inhibitors in this investigation suggests that these compounds will accumulate in the plasma membrane. Thus, it is possible that these compounds bind to an intramembraneous site, similar to that suggested for substrate binding to P-gp.

However, since most of the sequence homology between ABC transporters from different subfamilies is found in the ATP-binding domain (25,31), it is also possible that the multi-specific inhibitors interact with this part of the protein. So far, direct binding to the ATP-binding domains of ABC transporters has only been studied for a limited number of compounds (65,76–78). Some evidence suggests that flavonoids such as quercetin and silymarin, which inhibited all three transporters in this study, and chrysin, genistein and apigenin, which inhibited P-gp and BCRP, interact with the ATP-binding domain in P-gp (65,66). Interestingly, silymarin and quercetin differ from the other multi-specific inhibitors in

this investigation by being less lipophilic ($\log D_{7.4}$=1.5 and 1.0, respectively, in comparison with the median lipophilicity of 4.5) (Table I). In addition, together with MK571, they differ from the other multi-specific inhibitors by carrying a negative charge at physiological pH. Therefore, it is possible that the ionized functional groups interact with the same amino acids as the negatively charged phosphate moiety in ATP. In contrast, the higher lipophilicities and neutral or positive ionization states of all the other multi-specific inhibitors suggest that these compounds interact with a site other than the ATP-binding site, possibly located in the membrane–protein interface. This hypothesis was supported by the results of our docking study, which showed that MK571 binds to the catalytic site of the human MRP1 ATP-binding domain, but the lipophilic multi-specific inhibitors chlorprothixene, loperamide and thioridazine do not (Fig. 7).

For P-gp, an intra-membranous inhibitor binding site may well be part of the substrate binding pocket. In fact, as many as 11 of the 19 multi-specific ABC transport inhibitors found in this study are reported as P-gp substrates in the University of Tokyo transporter database (50), confirming their interaction with the transport site. In contrast, for both BCRP and MRP2, only two substrates were found among the lipophilic multi-specific inhibitors whereas 5 (63%) and 3 (75%) of the specific inhibitors have been reported to be substrates (50). Furthermore, the lipophilicity of the reported BCRP and MRP2 substrates is generally lower than for P-gp substrates and for the multi-specific inhibitors, with median $\log D_{7.4}$ of 0.5 and −0.4 for BCRP and MRP2, respectively (Fig. 6B). This indicates that the average substrate for each of these two transporters is less likely to partition to the plasma membrane, and suggests that the BCRP and MRP2 substrate binding sites may be located in the domain of the transporters that extends into the cytosol. Site-directed mutagenesis studies in MRP2 and the closely related transporter MRP1 also support a cytosolic location of the substrate binding site (79,80). It is thus likely that an intra-membranous inhibitory binding site would be distinct from the BCRP and MRP2 substrate binding sites, in contrast to the situation in P-gp (30,35).

Differences between the binding sites were also indicated by the model of specific inhibitors for P-gp and BCRP. Specific inhibitors of BCRP generally contained more nitrogen atoms and aromatic functions than inhibitors which are specific for P-gp, indicating that hydrogen bond π–π or π–cation interactions may be important for specific binding to BCRP. The P-gp-specific inhibitors, on the other hand, contained many carbonyl oxygens that likely take part in the formation of hydrogen bonds. This is consistent with the hydrogen bond acceptor patterns in P-gp substrates and inhibitors observed by Seelig and co-workers (20,75).

CONCLUSION

By using a global dataset representing the chemical space of orally administered drugs, we evaluated the inhibition specificity of the human ABC transporters P-gp, BCRP and MRP2. This resulted in the identification of 19 completely overlapping and 23 specific inhibitors. The concentration range of specificity was determined for haloperidol, prazosin and bromosulfalein, which were shown to be P-gp, BCRP and MRP2 specific, respectively. Control experiments verified that the well established P-gp/BCRP and BCRP inhibitors GF120918 and Ko143 are specific within defined concentration intervals, but revealed that MK571, commonly used as an MRP specific inhibitor, has comparable affinities for all three transporters. Virtual docking to a crystal structure of the ATP binding domain showed that the negatively charged and relatively hydrophilic MK571 interacts with the ATP catalytic site, but a set of highly lipophilic multi-specific inhibitors do not. A computational model for predicting general ABC transporter inhibition was developed from easily interpreted molecular descriptors. The model shows ABC transporter inhibitors to be more lipophilic, more aromatic and larger than non-inhibitors and correctly classified 79% and 80% of the inhibitors and non-inhibitors, respectively, in an external test set. In summary, we identified both specific inhibitors, which can be used to delineate transport processes in complex experimental systems, and multi-specific inhibitors, which are useful in primary ABC transporter screening in drug discovery settings. Our results highlight the importance of considering the specificity patterns of inhibitors used in drug transport studies.

ACKNOWLEDGEMENTS

This work was supported by the Swedish Research Council (Grant 9478), the Knut and Alice Wallenberg Foundation, the Swedish Fund for Research without Animal Experiments, and the Swedish Animal Welfare Agency.

REFERENCES

1. Borst P, Elferink RO. Mammalian ABC transporters in health and disease. Annu Rev Biochem. 2002;71:537–92. doi:10.1146/annurev.biochem.71.102301.093055.
2. Glavinas H, Krajcsi P, Cserepes J, Sarkadi B. The role of ABC transporters in drug resistance, metabolism and toxicity. Curr Drug Deliv. 2004;1:27–42. doi:10.2174/1567201043480036.
3. Krishnamurthy P, Schuetz JD. Role of ABCG2/BCRP in biology and medicine. Annu Rev Pharmacol Toxicol. 2006;46:381–410. doi:10.1146/annurev.pharmtox.46.120604.141238.
4. Borst P, Zelcer N, van de Wetering K. MRP2 and 3 in health and disease. Cancer Lett. 2006;234:51–61. doi:10.1016/j.canlet.2005.05.051.
5. Dietrich CG, Geier A, Oude Elferink RP. ABC of oral bioavailability: transporters as gatekeepers in the gut. Gut 2003;52:1788–95. doi:10.1136/gut.52.12.1788.
6. Hilgendorf C, Ahlin G, Seithel A, Artursson P, Ungell AL, Karlsson J. Expression of thirty-six drug transporter genes in human intestine, liver, kidney, and organotypic cell lines. Drug Metab Dispos. 2007;35:1333–40. doi:10.1124/dmd.107.014902.
7. Maliepaard M, Scheffer GL, Faneyte IF, van Gastelen MA, Pijnenborg AC, Schinkel AH, *et al.* Subcellular localization and distribution of the breast cancer resistance protein transporter in normal human tissues. Cancer Res. 2001;61:3458–64.
8. Harris MJ, Kuwano M, Webb M, Board PG. Identification of the apical membrane-targeting signal of the multidrug resistance-associated protein 2 (MRP2/MOAT). J Biol Chem. 2001;276:20876–81. doi:10.1074/jbc.M010566200.
9. Thiebaut F, Tsuruo T, Hamada H, Gottesman MM, Pastan I, Willingham MC. Cellular localization of the multidrug-resistance gene product P-glycoprotein in normal human tissues. Proc Natl Acad Sci U S A. 1987;84:7735–8. doi:10.1073/pnas.84.21.7735.
10. Tang W. Drug metabolite profiling and elucidation of drug-induced hepatotoxicity. Expert Opin Drug Metab Toxicol. 2007;3:407–20. doi:10.1517/17425255.3.3.407.

11. Smitherman PK, Townsend AJ, Kute TE, Morrow CS. Role of multidrug resistance protein 2 (MRP2, ABCC2) in alkylating agent detoxification: MRP2 potentiates glutathione S-transferase A1-1-mediated resistance to chlorambucil cytotoxicity. J Pharmacol Exp Ther. 2004;308:260–7. doi:10.1124/jpet.103.057729.
12. Morimoto K, Nakakariya M, Shirasaka Y, Kakinuma C, Fujita T, Tamai I, *et al.* Oseltamivir (Tamiflu) efflux transport at the blood–brain barrier via P-glycoprotein. Drug Metab Dispos. 2008;36:6–9. doi:10.1124/dmd.107.017699.
13. Schinkel AH, Wagenaar E, Mol CA, van Deemter L. P-glycoprotein in the blood–brain barrier of mice influences the brain penetration and pharmacological activity of many drugs. J Clin Invest. 1996;97:2517–24. doi:10.1172/JCI118699.
14. Kraemer J, Klein J, Lubetsky A, Koren G. Perfusion studies of glyburide transfer across the human placenta: implications for fetal safety. Am J Obstet Gynecol. 2006;195:270–4. doi:10.1016/j.ajog.2005.12.005.
15. Leslie EM, Deeley RG, Cole SP. Multidrug resistance proteins: role of P-glycoprotein, MRP1, MRP2, and BCRP (ABCG2) in tissue defense. Toxicol Appl Pharmacol. 2005;204:216–37. doi:10.1016/j.taap.2004.10.012.
16. Pavek P, Fendrich Z, Staud F, Malakova J, Brozmanova H, Laznicek M, *et al.* Influence of P-glycoprotein on the transplacental passage of cyclosporine. J Pharm Sci. 2001;90:1583–92. doi:10.1002/jps.1108.
17. Ambudkar SV, Kimchi-Sarfaty C, Sauna ZE, Gottesman MM. P-glycoprotein: from genomics to mechanism. Oncogene 2003;22:7468–85. doi:10.1038/sj.onc.1206948.
18. Crivori P, Reinach B, Pezzetta D, Poggesi I. Computational models for identifying potential P-glycoprotein substrates and inhibitors. Mol Pharm. 2006;3:33–44. doi:10.1021/mp050071a.
19. Ekins S, Kim RB, Leake BF, Dantzig AH, Schuetz EG, Lan LB, *et al.* Application of three-dimensional quantitative structure–activity relationships of P-glycoprotein inhibitors and substrates. Mol Pharmacol. 2002;61:974–81. doi:10.1124/mol.61.5.974.
20. Seelig A. A general pattern for substrate recognition by P-glycoprotein. Eur J Biochem. 1998;251:252–61. doi:10.1046/j.1432-1327.1998.2510252.x.
21. Pajeva IK, Wiese M. Pharmacophore model of drugs involved in P-glycoprotein multidrug resistance: explanation of structural variety (hypothesis). J Med Chem. 2002;45:5671–86. doi:10.1021/jm020941h.
22. Shapiro AB, Ling V. Positively cooperative sites for drug transport by P-glycoprotein with distinct drug specificities. Eur J Biochem. 1997;250:130–7. doi:10.1111/j.1432-1033.1997.00130.x.
23. Ambudkar SV, Kim IW, Sauna ZE. The power of the pump: mechanisms of action of P-glycoprotein (ABCB1). Eur J Pharm Sci. 2006;27:392–400. doi:10.1016/j.ejps.2005.10.010.
24. Sauna ZE, Andrus MB, Turner TM, Ambudkar SV. Biochemical basis of polyvalency as a strategy for enhancing the efficacy of P-glycoprotein (ABCB1) modulators: stipiamide homodimers separated with defined-length spacers reverse drug efflux with greater efficacy. Biochemistry 2004;43:2262–71. doi:10.1021/bi035965k.
25. Higgins CF. Multiple molecular mechanisms for multidrug resistance transporters. Nature 2007;446:749–57. doi:10.1038/nature05630.
26. McDevitt CA, Collins RF, Conway M, Modok S, Storm J, Kerr ID, *et al.* Purification and 3D structural analysis of oligomeric human multidrug transporter ABCG2. Structure 2006;14:1623–32. doi:10.1016/j.str.2006.08.014.
27. Rosenberg MF, Callaghan R, Modok S, Higgins CF, Ford RC. Three-dimensional structure of P-glycoprotein: the transmembrane regions adopt an asymmetric configuration in the nucleotide-bound state. J Biol Chem. 2005;280:2857–62. doi:10.1074/jbc.M410296200.
28. O'Mara ML, Tieleman DP. P-glycoprotein models of the apo and ATP-bound states based on homology with Sav1866 and MalK. FEBS Lett. 2007;581:4217–22. doi:10.1016/j.febslet.2007.07.069.
29. Sakurai A, Onishi Y, Hirano H, Seigneuret M, Obanayama K, Kim G, *et al.* Quantitative structure–activity relationship analysis and molecular dynamics simulation to functionally validate nonsynonymous polymorphisms of human ABC transporter ABCB1 (P-glycoprotein/MDR1). Biochemistry 2007;46:7678–93. doi:10.1021/bi700330b.
30. Omote H, Al-Shawi MK. Interaction of transported drugs with the lipid bilayer and P-glycoprotein through a solvation exchange mechanism. Biophys J. 2006;90:4046–59. doi:10.1529/biophysj.105.077743.
31. Shilling RA, Venter H, Velamakanni S, Bapna A, Woebking B, Shahi S, *et al.* New light on multidrug binding by an ATP-binding-cassette transporter. Trends Pharmacol Sci. 2006;27:195–203. doi:10.1016/j.tips.2006.02.008.
32. Pleban K, Kopp S, Csaszar E, Peer M, Hrebicek T, Rizzi A, *et al.* P-glycoprotein substrate binding domains are located at the transmembrane domain/transmembrane domain interfaces: a combined photoaffinity labeling-protein homology modeling approach. Mol Pharmacol. 2005;67:365–74. doi:10.1124/mol.104.006973.
33. Pajeva IK, Globisch C, Wiese M. Structure–function relationships of multidrug resistance P-glycoprotein. J Med Chem. 2004;47:2523–33. doi:10.1021/jm031009p.
34. Gatlik-Landwojtowicz E, Äänismaa P, Seelig A. Quantification and characterization of P-glycoprotein–substrate interactions. Biochemistry 2006;45:3020–32. doi:10.1021/bi051380+.
35. Gottesman MM, Pastan I. Biochemistry of multidrug resistance mediated by the multidrug transporter. Annu Rev Biochem. 1993;62:385–427. doi:10.1146/annurev.bi.62.070193.002125.
36. Matsson P, Englund G, Ahlin G, Bergström CA, Norinder U, Artursson P. A global drug inhibition pattern for the human ABC transporter BCRP (ABCG2). J Pharmacol Exp Ther. 2007;323:19–30. doi:10.1124/jpet.107.124768.
37. Pedersen JM, Matsson P, Bergström CA, Norinder U, Hoogstraate J, Artursson P. Prediction and identification of drug interactions with the human ATP-binding cassette transporter multidrug-resistance associated protein 2 (MRP2; ABCC2). J Med Chem. 2008;51:3275–87. doi:10.1021/jm7015683.
38. Zelcer N, Huisman MT, Reid G, Wielinga P, Breedveld P, Kuil A, *et al.* Evidence for two interacting ligand binding sites in human multidrug resistance protein 2 (ATP binding cassette C2). J Biol Chem. 2003;278:23538–44. doi:10.1074/jbc.M303504200.
39. Breedveld P, Pluim D, Cipriani G, Wielinga P, van Tellingen O, Schinkel AH, *et al.* The effect of Bcrp1 (Abcg2) on the *in vivo* pharmacokinetics and brain penetration of imatinib mesylate (Gleevec): implications for the use of breast cancer resistance protein and P-glycoprotein inhibitors to enable the brain penetration of imatinib in patients. Cancer Res. 2005;65:2577–82. doi:10.1158/0008-5472.CAN-04-2416.
40. Tian X, Li J, Zamek-Gliszczynski MJ, Bridges AS, Zhang P, Patel NJ, *et al.* Roles of P-glycoprotein, Bcrp, and Mrp2 in biliary excretion of spiramycin in mice. Antimicrob Agents Chemother. 2007;51:3230–4. doi:10.1128/AAC.00082-07.
41. Su Y, Lee SH, Sinko PJ. Inhibition of efflux transporter ABCG2/BCRP does not restore mitoxantrone sensitivity in irinotecan-selected human leukemia CPT-K5 cells: evidence for multifactorial multidrug resistance. Eur J Pharm Sci. 2006;29:102–10. doi:10.1016/j.ejps.2006.06.001.
42. Janneh O, Owen A, Chandler B, Hartkoorn RC, Hart CA, Bray PG, *et al.* Modulation of the intracellular accumulation of saquinavir in peripheral blood mononuclear cells by inhibitors of MRP1, MRP2, P-gp and BCRP. Aids 2005;19:2097–102. doi:10.1097/01.aids.0000194793.36175.40.
43. Huang L, Wang Y, Grimm S. ATP-dependent transport of rosuvastatin in membrane vesicles expressing breast cancer resistance protein. Drug Metab Dispos. 2006;34:738–42. doi:10.1124/dmd.105.007534.
44. Volk EL, Schneider E. Wild-type breast cancer resistance protein (BCRP/ABCG2) is a methotrexate polyglutamate transporter. Cancer Res. 2003;63:5538–43.
45. Suzuki M, Suzuki H, Sugimoto Y, Sugiyama Y. ABCG2 transports sulfated conjugates of steroids and xenobiotics. J Biol Chem. 2003;278:22644–9. doi:10.1074/jbc.M212399200.
46. Rabindran SK, He H, Singh M, Brown E, Collins KI, Annable T, *et al.* Reversal of a novel multidrug resistance mechanism in human colon carcinoma cells by fumitremorgin C. Cancer Res. 1998;58:5850–8.
47. Bergström CA, Wassvik CM, Norinder U, Luthman K, Artursson P. Global and local computational models for aqueous solubility prediction of drug-like molecules. J Chem Inf Comput Sci. 2004;44:1477–88. doi:10.1021/ci049909h.

48. Coan KE, Shoichet BK. Stoichiometry and physical chemistry of promiscuous aggregate-based inhibitors. J Am Chem Soc. 2008;130:9606–12. doi:10.1021/ja802977h.
49. Wierdl M, Wall A, Morton CL, Sampath J, Danks MK, Schuetz JD, *et al.* Carboxylesterase-mediated sensitization of human tumor cells to CPT-11 cannot override ABCG2-mediated drug resistance. Mol Pharmacol. 2003;64:279–88. doi:10.1124/mol.64.2.279.
50. Ozawa N, Shimizu T, Morita R, Yokono Y, Ochiai T, Munesada K, *et al.* Transporter database, TP-Search: a web-accessible comprehensive database for research in pharmacokinetics of drugs. Pharm Res. 2004;21:2133–4. doi:10.1023/B:PHAM.0000048207.11160.d0.
51. Polli JW, Wring SA, Humphreys JE, Huang L, Morgan JB, Webster LO, *et al.* Rational use of *in vitro* P-glycoprotein assays in drug discovery. J Pharmacol Exp Ther. 2001;299:620–8.
52. Taipalensuu J, Tavelin S, Lazorova L, Svensson AC, Artursson P. Exploring the quantitative relationship between the level of MDR1 transcript, protein and function using digoxin as a marker of MDR1-dependent drug efflux activity. Eur J Pharm Sci. 2004;21:69–75. doi:10.1016/S0928-0987(03)00204-5.
53. Englund G, Hallberg P, Artursson P, Michaelsson K, Melhus H. Association between the number of coadministered P-glycoprotein inhibitors and serum digoxin levels in patients on therapeutic drug monitoring. BMC Med. 2004;2:E8. doi:10.1186/1741-7015-2-8.
54. Adachi Y, Suzuki H, Sugiyama Y. Comparative studies on *in vitro* methods for evaluating *in vivo* function of MDR1 P-glycoprotein. Pharm Res. 2001;18:1660–68. doi:10.1023/A:1013358126640.
55. Hunter J, Hirst BH, Simmons NL. Drug absorption limited by P-glycoprotein-mediated secretory drug transport in human intestinal epithelial Caco-2 cell layers. Pharm Res. 1993;10:743–9. doi:10.1023/A:1018972102702.
56. Matsson P, Bergström CA, Nagahara N, Tavelin S, Norinder U, Artursson P. Exploring the role of different drug transport routes in permeability screening. J Med Chem. 2005;48:604–13. doi:10.1021/jm049711o.
57. Palm K, Stenberg P, Luthman K, Artursson P. Polar molecular surface properties predict the intestinal absorption of drugs in humans. Pharm Res. 1997;14:568–71. doi:10.1023/A:1012188625088.
58. Tarini M, Cignoni P, Montani C. Ambient occlusion and edge cueing to enhance real time molecular visualization. IEEE Trans Vis Comput Graph 2006;12:1237–44. doi:10.1109/TVCG.2006.115.
59. Gupta A, Zhang Y, Unadkat JD, Mao Q. HIV protease inhibitors are inhibitors but not substrates of the human breast cancer resistance protein (BCRP/ABCG2). J Pharmacol Exp Ther. 2004;310:334–41. doi:10.1124/jpet.104.065342.
60. Bates SE, Robey R, Miyake K, Rao K, Ross DD, Litman T. The role of half-transporters in multidrug resistance. J Bioenerg Biomembr. 2001;33:503–11. doi:10.1023/A:1012879205914.
61. Gekeler V, Ise W, Sanders KH, Ulrich WR, Beck J. The leukotriene LTD4 receptor antagonist MK571 specifically modulates MRP associated multidrug resistance. Biochem Biophys Res Commun. 1995;208:345–52. doi:10.1006/bbrc.1995.1344.
62. Penzotti JE, Lamb ML, Evensen E, Grootenhuis PD. A computational ensemble pharmacophore model for identifying substrates of P-glycoprotein. J Med Chem. 2002;45:1737–40. doi:10.1021/jm0255062.
63. Ramaen O, Leulliot N, Sizun C, Ulryck N, Pamlard O, Lallemand JY, *et al.* Structure of the human multidrug resistance protein 1 nucleotide binding domain 1 bound to Mg2+/ATP reveals a non-productive catalytic site. J Mol Biol. 2006;359:940–9. doi:10.1016/j.jmb.2006.04.005.
64. Leier I, Jedlitschky G, Buchholz U, Cole SP, Deeley RG, Keppler D. The MRP gene encodes an ATP-dependent export pump for leukotriene C4 and structurally related conjugates. J Biol Chem. 1994;269:27807–10.
65. Conseil G, Baubichon-Cortay H, Dayan G, Jault JM, Barron D, Di Pietro A. Flavonoids: a class of modulators with bifunctional interactions at vicinal ATP- and steroid-binding sites on mouse P-glycoprotein. Proc Natl Acad Sci U S A. 1998;95:9831–6. doi:10.1073/pnas.95.17.9831.
66. de Wet H, McIntosh DB, Conseil G, Baubichon-Cortay H, Krell T, Jault JM, *et al.* Sequence requirements of the ATP-binding site within the C-terminal nucleotide-binding domain of mouse P-glycoprotein: structure–activity relationships for flavonoid binding. Biochemistry 2001;40:10382–91. doi:10.1021/bi010657c.
67. Allen JD, van Loevezijn A, Lakhai JM, van der Valk M, van Tellingen O, Reid G, *et al.* Potent and specific inhibition of the breast cancer resistance protein multidrug transporter *in vitro* and in mouse intestine by a novel analogue of fumitremorgin C. Mol Cancer Ther. 2002;1:417–25.
68. de Bruin M, Miyake K, Litman T, Robey R, Bates SE. Reversal of resistance by GF120918 in cell lines expressing the ABC half-transporter, MXR. Cancer Lett. 1999;146:117–26. doi:10.1016/S0304-3835(99)00182-2.
69. Bow DA, Perry JL, Miller DS, Pritchard JB, Brouwer KL. Localization of P-gp (Abcb1) and Mrp2 (Abcc2) in freshly isolated rat hepatocytes. Drug Metab Dispos. 2008;36:198–202. doi:10.1124/dmd.107.018200.
70. Hewitt NJ, Lechon MJ, Houston JB, Hallifax D, Brown HS, Maurel P, *et al.* Primary hepatocytes: current understanding of the regulation of metabolic enzymes and transporter proteins, and pharmaceutical practice for the use of hepatocytes in metabolism, enzyme induction, transporter, clearance, and hepatotoxicity studies. Drug Metab Rev. 2007;39:159–234. doi:10.1080/03602530601093489.
71. Ahlin G, Karlsson J, Pedersen JM, Gustavsson L, Larsson R, Matsson P, *et al.* Structural requirements for drug inhibition of the liver specific human organic cation transport protein 1. J Med Chem. 2008;51:5932–42. doi:10.1021/jm8003152.
72. Cui Y, König J, Leier I, Buchholz U, Keppler D. Hepatic uptake of bilirubin and its conjugates by the human organic anion transporter SLC21A6. J Biol Chem. 2001;276:9626–30. doi:10.1074/jbc.M004968200.
73. LeCluyse EL, Alexandre E, Hamilton GA, Viollon-Abadie C, Coon DJ, Jolley S, *et al.* Isolation and culture of primary human hepatocytes. Methods Mol Biol. 2005;290:207–29.
74. Sasaki M, Suzuki H, Aoki J, Ito K, Meier PJ, Sugiyama Y. Prediction of *in vivo* biliary clearance from the *in vitro* transcellular transport of organic anions across a double-transfected Madin-Darby canine kidney II monolayer expressing both rat organic anion transporting polypeptide 4 and multidrug resistance associated protein 2. Mol Pharmacol. 2004;66:450–9. doi:10.1124/mol.66.2.330.
75. Seelig A, Landwojtowicz E. Structure–activity relationship of P-glycoprotein substrates and modifiers. Eur J Pharm Sci. 2000;12:31–40. doi:10.1016/S0928-0987(00)00177-9.
76. Pezza RJ, Villarreal MA, Montich GG, Argarana CE. Vanadate inhibits the ATPase activity and DNA binding capability of bacterial MutS. A structural model for the vanadate-MutS interaction at the Walker A motif. Nucleic Acids Res. 2002;30:4700–8. doi:10.1093/nar/gkf606.
77. Oloo EO, Tieleman DP. Conformational transitions induced by the binding of MgATP to the vitamin B12 ATP-binding cassette (ABC) transporter BtuCD. J Biol Chem. 2004;279:45013–9. doi:10.1074/jbc.M405084200.
78. Moran O, Galietta LJ, Zegarra-Moran O. Binding site of activators of the cystic fibrosis transmembrane conductance regulator in the nucleotide binding domains. Cell Mol Life Sci. 2005;62:446–60. doi:10.1007/s00018-004-4422-3.
79. Bakos E, Homolya L. Portrait of multifaceted transporter, the multidrug resistance-associated protein 1 (MRP1/ABCC1). Pflugers Arch. 2007;453:621–41. doi:10.1007/s00424-006-0160-8.
80. Letourneau IJ, Slot AJ, Deeley RG, Cole SP. Mutational analysis of a highly conserved proline residue in MRP1, MRP2, and MRP3 reveals a partially conserved function. Drug Metab Dispos. 2007;35:1372–9. doi:10.1124/dmd.107.015479.